Hindawi
Adsorption Science & Technology
Volume 2023, Article ID 5305732, 9 pages
https://doi.org/10.1155/2023/5305732

Research Article

# Thermal Adsorption and Corrosion Characteristic Study of Copper Hybrid Nanocomposite Synthesized by Powder Metallurgy Route

**V. Senthilkumar,[1] A. Nagadeepan,[1] Melvin Victor De Poures,[2] R. Sasikumar,[3] N. Mukilarasan,[4] M. Aruna,[5] C. B. Priya,[6] Gopal Kaliyaperumal,[7] and Elangomathavan Ramaraj[8]**

[1]Department of Mechanical Engineering, SRM TRP Engineering College, Trichy, 621105 Tamil Nadu, India
[2]Department of Thermal Engineering, Saveetha School of Engineering, SIMATS, Chennai, 602105 Tamil Nadu, India
[3]Department of Mechanical Engineering, Erode Sengunthar Engineering College, Erode, 638057 Tamil Nadu, India
[4]Department of Mechanical Engineering, Jeppiaar Institute of Technology, Chennai, 631604 Tamil Nadu, India
[5]Faculty of Mechanical and Industrial Engineering, Liwa College of Technology, Abu Dhabi, UAE
[6]Department of Mechanical Engineering, OASYS Institute of Technology, Trichy, 621006 Tamil Nadu, India
[7]Department of Mechanical Engineering, New Horizon College of Engineering, Bengaluru, Karnataka 560103, India
[8]Department of Biology, College of Natural and Computational Sciences, Debre Tabor University, Amhara Region, Ethiopia

Correspondence should be addressed to Elangomathavan Ramaraj; elanmath@dtu.edu.et

Received 20 October 2022; Revised 2 January 2023; Accepted 20 March 2023; Published 30 March 2023

Academic Editor: Debabrata Barik



Novel constitutions of ceramic bond the new opportunity of engineering materials via solid-state process attaining enhanced material characteristics to overcome the drawback of conventional materials used in aquatic applications. The copper-based materials have great potential to explore high corrosion resistance and good thermal performance in the above applications. The main objectives of this research are to develop and enhance the characteristics of the copper-based hybrid nanocomposite containing different weight percentages of alumina and graphite hard ceramics synthesized via solid-state processing (powder metallurgy). The presence of alumina nanoparticles with a good blending process has to improve the corrosion resistance, and graphite nanoparticles may limit the weight loss of the sample during potentiodynamic corrosion analysis. The developed composite's micro Vickers hardness is evaluated by the E384 standard on ASTM value of 69 Hv and is noted by increasing the weight percentages of alumina nanoparticles. The conduction temperature of actual sintering anticipates the thermogravimetric analysis of developed composite samples varied from 400°C to 750°C. The thermogravimetric graph illustration curve of the tested sample found double-step decomposition identified between 427°C and 456°C. The potentiodynamic analyzer is used to evaluate the corrosion behaviour of the sample and the weight loss equation adopted for finding the theoretical weight loss of the composite.

## 1. Introduction

Copper is one of the best corrosion-free metals in defense and aquatic applications. Naturally, it is ductile, has good fluidity, and exhibits high thermal and electrical conductivity compared to traditional metals [1]. In addition, copper-based composite materials can serve extensive performance in the automotive and electronic industries due to their excellent thermal, tribological, mechanical, electrical, and corrosion characteristics [2–5]. The secondary phase materials based on ceramics are used to create copper composite. It offers the specific desired characteristics with economic [6, 7]. The drawback behind the fabrication of copper/ceramic composite is poor bonding on inferior wetting properties [8, 9]. To solve the above, more than one suitable secondary phase reinforcement has been adopted in a similar composite in the form of nano- or

Table 1: Properties of pure copper.

| Properties | Density | Vickers hardness | Tensile strength | Elongation at break | Coefficient of thermal expansion | Thermal conductivity | Melting point | Corrosion rate |
|---|---|---|---|---|---|---|---|---|
| Units | g/cc | Hv | MPa | % | $\mu$m/m°C | W/m·K | °C | mm/year |
| Value | 7.76 | 50 | 210 | 60 | 16.4 | 385 | 1083 | 0.001 |

Table 2: Properties of ceramics.

| Properties | Density (g/cc) | Hardness (Mohs) | Tensile modulus (GPa) | Coefficient of thermal expansion ($\mu$m/m°C) | Thermal conductivity (W/m·K) |
|---|---|---|---|---|---|
| Alumina | 3.96 | 9 | 370 | 0.6 | 30 |
| Graphite | 2.25 | 1 | 4.8 | 0.6-4.30 | 24 |

microparticles called hybrid nanocomposite. Recently, the growth hybrid composite materials developed with different matrix materials are incorporated with suitable secondary phase reinforcement materials that can prevent catastrophic and scuffing indemnity [10–13]. Many hybrid composites have been produced for various applications like sports goods, marine, automotive, structural, aviation, and defense [14–17]. However, the investigation results of increases in the tensile strength and hardness and a constrained coefficient of friction show that the composite created with a copper-based matrix and graphite particles can provide a solid lubricant effect. One additional ceramic phase, either aluminium oxide or silicon carbide, is considered to be a reinforcement [18, 19]. The above-referred ceramic has been influenced by copper's inherent conductivity and machinability [20]. The copper matrix with different secondary phase combinations is evaluated by a digital-type thermoanalyzer, resulting in better thermal conductivity. The majority of jet engines now have copper/ceramic combinations with good corrosion resistance [21]. At the earliest, chromium-reinforced copper matrix composite coated with carbon nanotubes found a problem with the wetting of secondary reinforcement [22].

The hybrid composite produced by two different ceramic particles is considered one in nanoscale and micron size via powder metallurgy. It results in superior strength of composite [23]. The corrosion behaviour of 1% carbon-reinforced Fe composite was evaluated by 1% of $HNO_3$ solution at 25 hours. It reveals that the corrosion rate on pure Fe was inversely higher than Fe/1% carbon composite [24]. The powder metallurgy route was developed with the waste ground nut of shell ash-reinforced Cu-WC hybrid composite. The results of the produced composite containing higher ground shell ash found increased corrosion resistance [25]. A seawater environment tested the corrosion performance of copper and its alloy via an electrochemical corrosion test. It was noticed with high corrosion resistance on both copper and its alloy [26]. The Al-Si alloy composite developed with alumina nanoparticles found increased corrosion resistance compared to cast Al-Si alloy. The corrosion resistance enhancement was mainly attributed to its Si constitutions with hard ceramic [27]. The mechanical alloying method was one of the best routes to obtain pore-free composites [28, 29]. The electrochemical corrosion test of copper-based composites found increased resistance value due to the effective blending of metal powder [30]. According to the recent research literature cited above from a variety of researchers, the development of a copper matrix composite, which is attracting more attention from the nanoscience community, could replace the microparticle size with a nanosize, improving the matrix's ability to resist corrosion. As a result, the current experimental inquiry focuses on heat adsorption, and the thermogravimetric and potentiodynamic analyses were used to examine the corrosion resistance behaviour of a copper hybrid nanocomposite made via powder metallurgy.

Table 3: Constitutions of copper hybrid nanocomposites.

| Sample no. | Copper in % | Alumina in % | Graphite in % |
|---|---|---|---|
| 1 | 93 | 2 | 5 |
| 2 | 93 | 4 | 3 |
| 3 | 93 | 6 | 1 |

## 2. Materials and Processing Details

*2.1. Choice of the Base Matrix.* In the present investigation, pure copper (varied particle size) is considered as the matrix material, and its properties are mentioned in Table 1. It consists of 99.5% copper with 0.5% of other constitutions helping to assist the thermal changes during the melting of copper [1, 2]. Pure copper facilities have good thermal, electrical, and wear properties [3–5].

*2.2. Choice of Reinforcements.* The alumina and graphite particles are considered for reinforcements with a particle size of 50 nm. Both ceramics are thermally stable at a higher temperature, provide good solid lubricant, resist scratch against the frictional force, and have good hardness [18, 20, 21]. The characteristics of nanoalumina and micrographite particles are tabulated in Table 2.

*2.3. Processing Details for Copper Hybrid Nanocomposites.* The constitutions of copper matrix and ceramic reinforcement details are referred to in Table 3. The required percentages of copper metal powder and its secondary bonding phase elements, such as alumina/graphite nanoparticles, are weighted by a digital weighing machine with the accuracy of ±0.001 grams as shown in Figures 1(a)–1(c).


Figure 1: Actual illustrations for (a) copper metal particles, (b) alumina nanoparticles, and (c) graphite nanoparticles.

Figure 2 represents the overall powder metallurgy process. Figure 2(a) shows the process layout for composite fabrication. The measured quantity of copper matrix and its ceramic (alumina/graphite) are blended at 500 rpm for 2 hours via a PM100 ball milling machine configured with a planetary ball setup, shown in Figure 2(b). The PM100 ball mill is easy to use for 8 kg mass and 220 ml for sample material. The blended materials are placed in air-sealed TiC-coated vessels that hold a few TiC-coated balls at a ratio of 10 : 1. (10: metal powder in grams and 1: number of TiC balls). It leads to an increase in particle compactness with uniform and homogenous particle distribution achieved. It helps to limit the micron size aggregation.

The blended metal powders are filled into circular die sizes of 50 mm in diameter. After that, it is compacted via a universal compact testing machine with an applied compressive force of 20 tons to make circular green pellets. Finally, the compacted green pellets are sintered by an induction furnace at the temperature of 700°C under a soaking period of 180 min. However, the sintering temperature of green pellets is lower than the melting point temperature of parent materials.

The mechanical and tribological properties of the sintered metal samples are improved, and oxidation is minimised when they are stored in a boiler to debond the moisture contents in an inert atmosphere [28, 31]. The developed composite samples are shown in Figure 2(c).

*2.4. Experimental Test Details.* The micro-Vickers hardness of advanced hybrid composites (E384) is estimated using the VM50 model apparatus by the ASTM standard via FIE. The ASTM-E384 standard prepared hybrid nanocomposite samples are tested by 70 grams load at 20-second time duration. The thermal behaviour of the polymer matrix composite is analyzed by thermogravimetric analysis. A potentiodynamic analyzer evaluated the corrosion studies of advanced composites, and the theoretical weight loss of the composite is identified by equation (1).

## 3. Results and Discussions

*3.1. Micro Vickers Hardness.* Figure 3 represents the micro Vickers hardness value of a copper hybrid nanocomposite containing alumina and graphite nanoparticles, followed by the ratio of 2 : 5, 4 : 3, and 6 : 1, respectively. The presence of 50 nm size alumina particles occupying a significant portion of the copper matrix results in an increased hardness value of the composite.

The addition of alumina nanoparticles to the copper matrix causes a rise in Vickers hardness number, which is measured as microhardness on the copper matrix [32]. It is revealed from Figure 3 that the Vickers hardness of copper hybrid nanocomposite linearly increases with an increase in alumina content, resulting in $58 \pm 0.5$ Hv, $64 \pm 0.71$ Hv, and $69 \pm 0.73$. The maximum hardness value of $69 \pm 0.73$ is observed by sample 3 (6 : 1). It was due to the presence of complex alumina nanoparticles that resist the indentation against the applied load. The hardness of sample 3 increased by 38% compared to cast copper. Similarly, the hardness of the hybrid composite was increased by 30% with the presence of $Si_3N_4/ZrO_2$ [17]. However, the presences of alumina and graphite nanoparticles in the copper matrix resist the indentation against the load applied and limit the dislocation of particle.

*3.2. Thermal Performance Studies*

*3.2.1. Thermogravimetric Analysis on Thermal Adsorption Properties for Copper Hybrid Nanocomposites.* The real sintering conduction temperature, which ranges from 400°C to 750°C over a certain time period, is used to evaluate the thermal performance on thermogravimetric analysis for the mass of copper hybrid nanocomposites including various percentages of alumina and graphite nanoparticles. This thermogravimetric estimation offered the physical changes for the composite phase transitions and decomposition during thermal changes. Substantial limits calculate the thermal adsorption on the thermal stability of copper hybrid nanocomposite. However, the insignificant mass loss on copper hybrid nanocomposite is not traced or shows a nonslope trace [33–35]. The differential temperature analysis (DTA), thermal-gravimetric analysis (TGA), and combinations of differential thermogravimetric (DTG) thermograph are used to study the thermal adsorption performance curve of copper hybrid nanocomposite samples 1, 2, and 3. The TGA, DTA, and DTG curves of a copper hybrid nanocomposite comprising ceramics in the ratios of 4 : 3 and 6 : 1 are shown in Figures 4(b) and 4(c). Sample 1 from Figure 4(a) represents the decompositions of copper hybrid nanocomposite containing 2 wt% alumina and 5% graphite nanoparticles lying in the 440°C to 480°C temperature range. Above 520°C temperature found the increased decomposition rate due to the dislocation of particles within the matrix. So

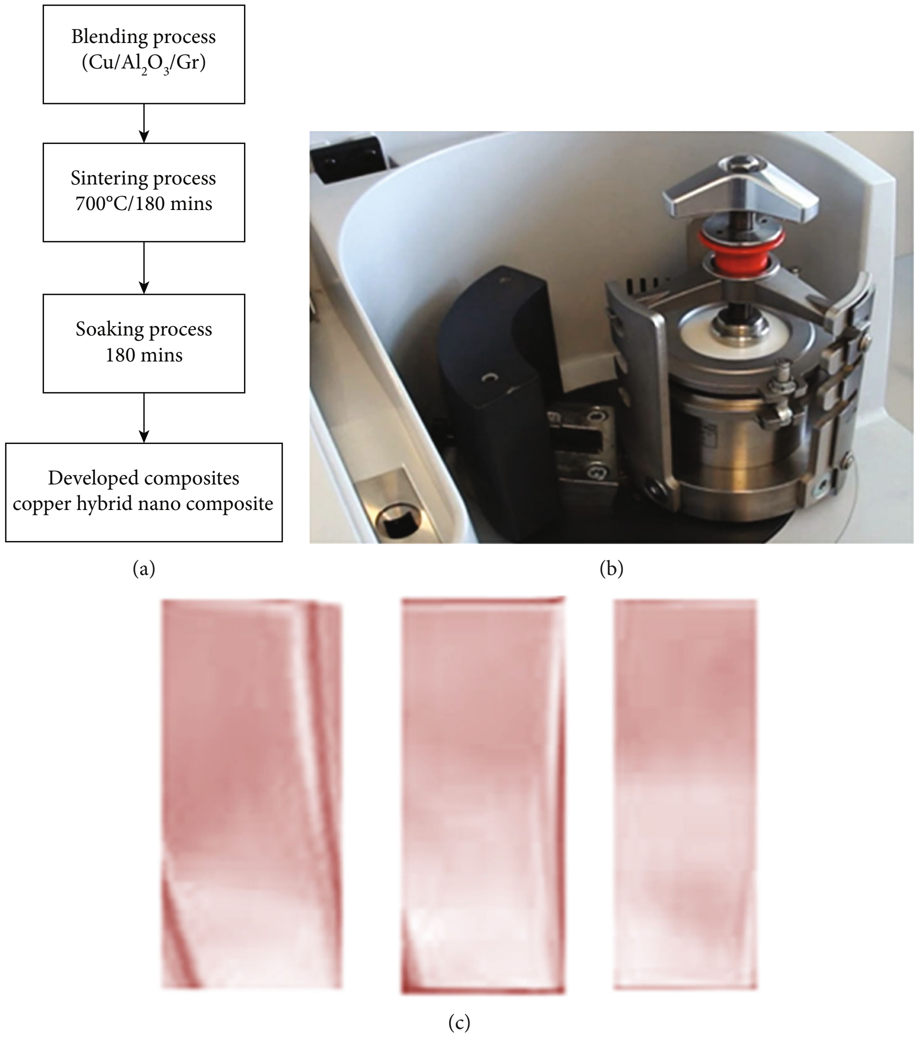


Figure 2: Overall powder metallurgy process: (a) process layout, (b) PM100 model planetary ball milling apparatus, and (c) developed composite samples.

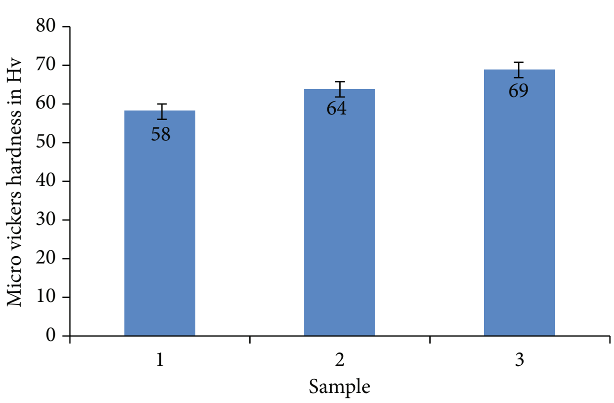


Figure 3: Micro Vickers hardness for copper hybrid nanocomposites.

the mass loss of the composite is hiked more than 600 micrograms. Figures 4(b) and 4(c) show the TGA, DTA, and DTG curves of copper hybrid nanocomposite containing the ceramic at ratios 4 : 3 and 6 : 1. Samples 2 and 3 show similar decomposition with minor slope variations due to irreversible ratio of alumina and graphite nanoparticles in the copper matrix. However, it is revealed from Figures 4(a)–4(c) that the thermograph of copper hybrid nanocomposites is accomplished with higher temperature variations and withstands the working temperature devoid of structural loss or damage. The entire test samples of thermal adsorption on hybrid nanocomposite are stable and show ±42°C adsorption temperature.

The results from Figures 4(a)–4(c) show a similar curve pattern on TGA, DTA, and DTG thermographs. Moreover, the content of 93% copper bonded with 6% alumina and 1% graphite shows optimum mass loss results during thermal adsorption of 5.18 mg at 236°C. Further increase in temperature above 250°C shows the intermediate zone to minimize the mass loss of 5.21 mg between 450°C and 471°C. The minimum mass on the thermal adsorption effect of copper hybrid nanocomposite was 5.39 mg at 723°C. It was a limited 18.78% mass loss compared to copper elements. However, the TGA-developed double-step curve on decomposition was identified between the temperature ranges of 427°C to 456°C. More than 300 micrograms increases the mass loss of the composite at the increased

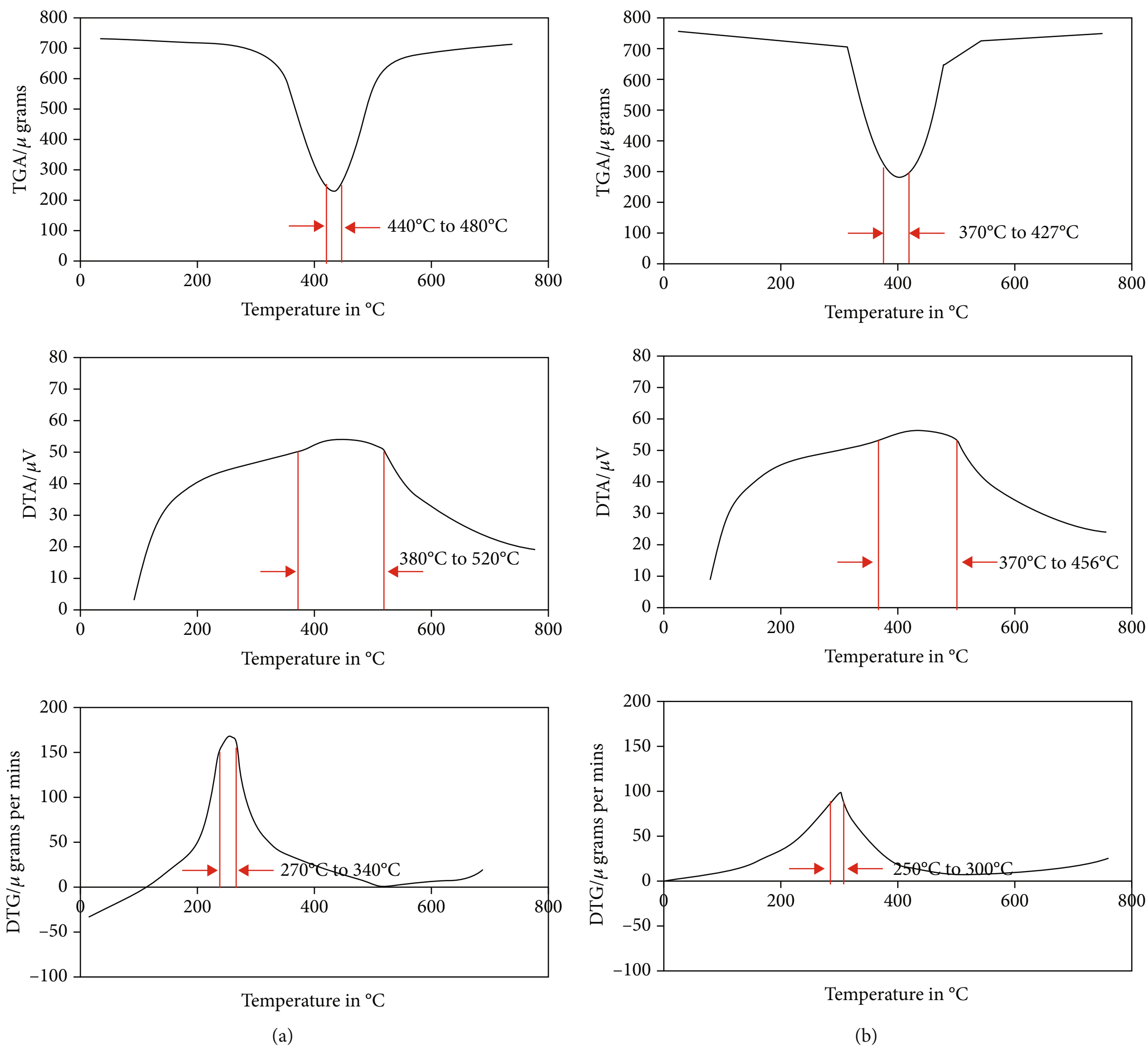


FIGURE 4: Continued.

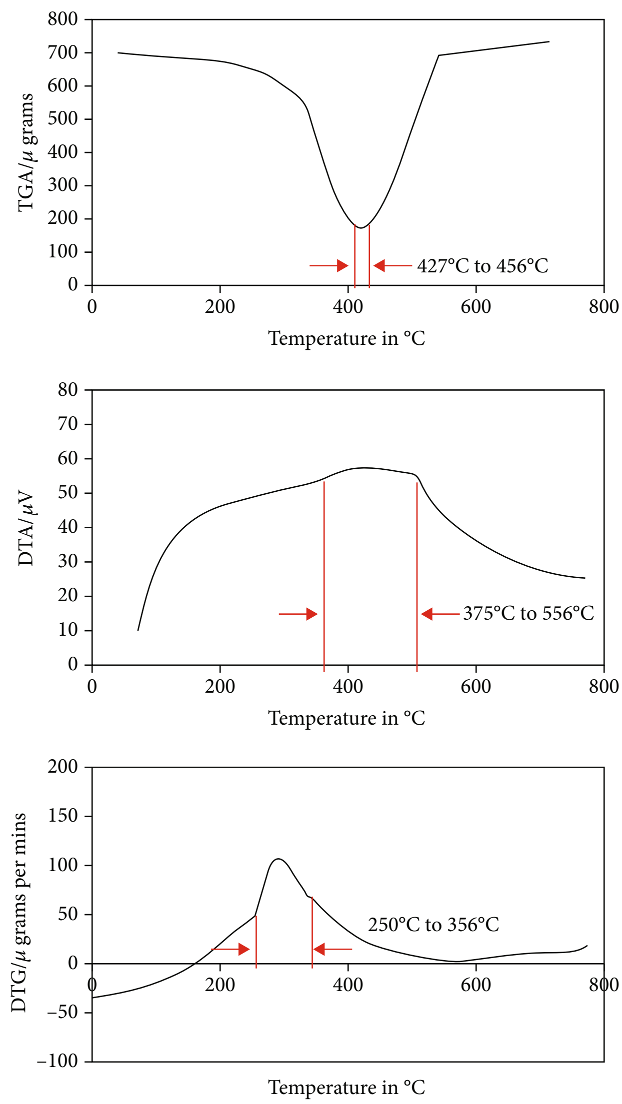


(c)

Figure 4: (a) Thermal adsorption effect on TGA, DTA, and DTG results for sample 1. (b) Thermal adsorption effect on TGA, DTA, and DTG results for sample 2. (c) Thermal adsorption effect on TGA, DTA, and DTG results for sample 3.

temperature of 427°C, as noted in Figure 4(b). Similarly, the composite contained 6 wt% alumina, and 1% graphite found an increased mass loss from 50 mg to 95 mg on improved temperature rise of 250°C to 356°C.

*3.3. Corrosion Performance.* In the present study, copper metal is considered a cathode polarity and easily permits the electron to oxidation. A base metal accomplishes the developed composites for aquatic applications. The solution medium of sodium chloride and sodium hydroxide evaluates the corrosion nature of multiceramic-reinforced copper matrix hybrid nanocomposites. The 1.5% of sodium hydroxide solution is diluted for 300 ml solution. It is held in a glass beaker. The copper matrix hybrid nanocomposite of corrosion samples is immersed in the sodium hydroxide solution for 1 day to study the potentiodynamic analysis. Figures 5(a)–5(c) illustrate the potentiodynamic analysis on corrosion studies of copper hybrid nanocomposites containing 2%, 4%, and 6% alumina. Correspondingly, the graphite nanoparticle incorporated with alumina is 5%, 3%, and 1%, respectively. The digital weighing machine with an accuracy of ±0.001 gram is utilized to measure the weight of the composite sample before ($W1$) and after ($W2$) corrosion study. The theoretical weight loss is calculated by

$$\text{Weight loss of composite} = \frac{W2 - W1}{W2}. \quad (1)$$

Figure 5 shows that a copper hybrid nanocomposite with 6% alumina and 1% graphite had the highest resistance to the development of corrosion. When compared to the anode pole, the cathode polarisation has greater corrosion resistance. Similarly, the prepared corrosion test samples are dipped in sea salt water, and the weight loss method estimates its effect on corrosion formation. The test result of the corrosion study is mentioned in Table 4. It was noted

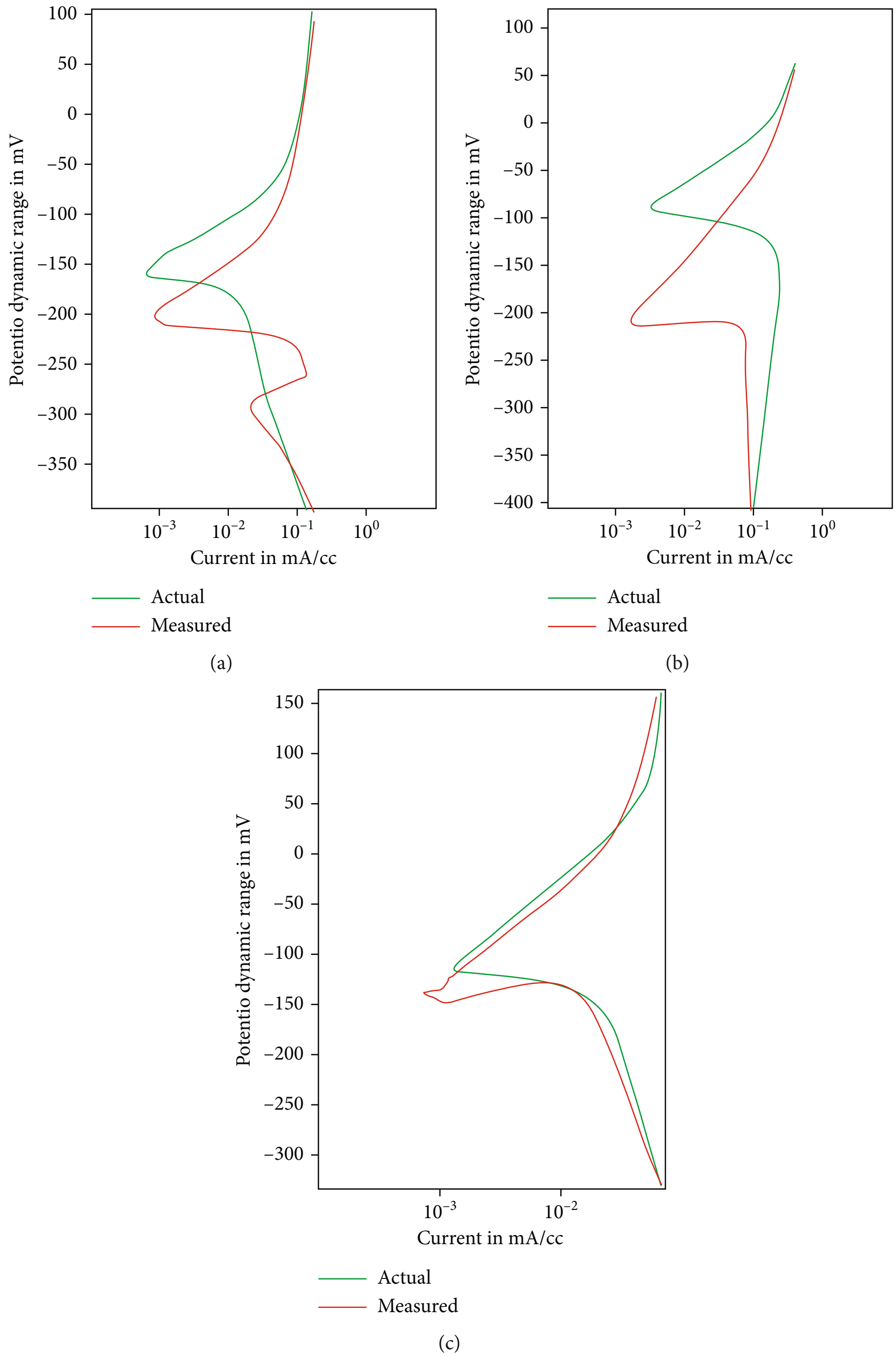


Figure 5: (a) Potentiodynamic analysis of corrosion results on sample 1. (b) Potentiodynamic analysis of corrosion results on sample 2. (c) Potentiodynamic analysis of corrosion results on sample 3.

Table 4: Corrosion test results.

| Sample | Sodium hydroxide solution | | | | Sea water | |
|---|---|---|---|---|---|---|
| | Initial weight (g) | pH concentration in g 0.75% | 0.50% | 0.25% | Initial weight (g) | Loss of weight (g) |
| 1 | 6 | 0.19 | 0.15 | 0.087 | 3 | 0.187 |
| 2 | 6 | 0.15 | 0.13 | 0.031 | 3 | 0.181 |
| 3 | 6 | 0.02 | 0 | 0 | 3 | 0 |

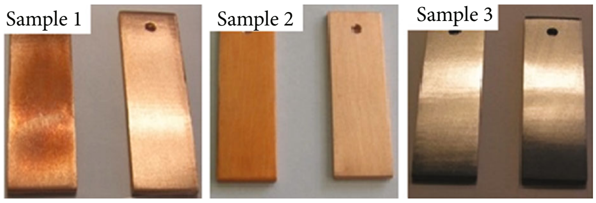


Figure 6: Corrosion test samples.

from Table 4 that sample 3 found intensive corrosion resistance with zero weight loss. It was due to the combination of copper/alumina/graphite. The alumina content resists the corrosion support on the copper matrix, and graphite limits weight loss.

It is observed from Figure 5(a) that the potentiodynamic analysis curve for sample 1 is not similar to the actual representation. The line of green represents the actual curve before the corrosion test, and the red curve indicates the curve for corrosion sample 1. There are few changes found in the potential curve. Sample 1 is not suitable for the above applications. It has some minor corrosion-affected areas to be deflected.

Figure 5(b) represents the potentiodynamic analysis of corrosion results on sample 2 copper hybrid nanocomposites. The potential pattern for both actual and measured values shows a similar pattern, but the measured corrosion value deviates from the actual value. It has represented some corrosion-affected places during the evaluation of sodium hydroxide solution for 1 day. It may lead to damage to the copper matrix hybrid nanocomposites. The proof of pH concentration is mentioned in Table 4.

Figure 5(c) shows the potentiodynamic analysis curve on corrosion results on sample 3 hybrid nanocomposite. The actual and measured corrosion curves match similarly with a few variations. This demonstrates that sample 3's corrosion analysis resulted in no material loss. The measured corrosion value of sample 3 is represented in Table 4 with varied pH concentrations. The tested samples are shown in Figure 6.

## 4. Conclusions

The copper-based hybrid nanocomposite is effectively developed with alumina and graphite nanoparticles through the powder metallurgy route. The developed hybrid nanocomposites are subjected to hardness; thermal adsorption behaviour on TGA, DTA, and DTG routes; and corrosion studies. The following conclusions are made as follows:

(i) The presence of nanoalumina and graphite ceramics enhances the characteristics of hybrid nanocomposite, and its experimental results are proven

(ii) There is a progressive improvement in hardness, effective thermal performance, and good corrosion resistance

(iii) Sample 3 (Cu/6% $Al_2O_3$/1% graphite) found a superior hardness of $69 \pm 0.73$ and increased 38% of cast copper material

(iv) The intermediate thermal stability of the composite (sample 3) was identified as 5.21 mg between 450°C and 471°C

(v) The corrosion studies found that the increased alumina content in the copper matrix shows an exhibited corrosion resistance value. There is no significant loss of composite during the potentiodynamic analysis

## Data Availability

All the data required are available within the manuscript.

## Conflicts of Interest

The authors declare no conflicts of interest.

## References

[1] C. A. Loto, "Electrochemical noise evaluation and data statistical analysis of stressed aluminium alloy in NaCl solution," *Journal of Alexandria Engineering Journal*, vol. 57, no. 3, pp. 1313–1321, 2018.

[2] S. Mallik, N. Ekere, C. Best, and R. Bhatti, "Investigation of thermal management materials for automotive electronic control units," *Applied Thermal Engineering*, vol. 31, no. 2-3, pp. 355–362, 2011.

[3] R. Zitoune, M. el Mansori, and V. Krishnaraj, "Tribo-functional design of double cone drill implications in tool wear during drilling of copper mesh/CFRP/woven ply," *Wear*, vol. 302, no. 1-2, pp. 1560–1567, 2013.

[4] S. Kumari, A. Kumar, P. R. Sengupta, P. K. Dutta, and R. B. Mathur, "Improving the mechanical and thermal properties of semi-coke based carbon/copper composites reinforced using carbon nanotubes," *Journal of Advanced Material Letter*, vol. 5, no. 5, pp. 265–271, 2014.

[5] M. Vivekanandan, M. Premalatha, N. Anantharaman, and R. Venkatesh, "Hydrodynamic studies of CFBC boiler with three types of air distributor nozzles: experimental and CFD analysis," *Journal of Thermal Analysis and Calorimetry*, vol. 148, no. 2, pp. 405–415, 2023.

[6] M. Yusoff, R. Othman, and Z. Hussain, "Mechanical alloying and sintering of nanostructured tungsten carbide- reinforced copper composite and its characterization," *Material Design*, vol. 32, no. 6, pp. 3293–3298, 2011.

[7] A. A. Thakre and S. Soni, "Modeling of burr size in drilling of aluminum silicon carbide composites using response surface methodology," *Engineering Science and Technology*, vol. 19, no. 3, pp. 1199–1205, 2016.

[8] S. F. Moustafa, Z. Abdel-Hamid, and A. M. Abd-Elhay, "Copper matrix SiC and $Al_2O_3$ particulate composites by powder metallurgy technique," *Material Letter*, vol. 53, no. 4-5, pp. 244–249, 2002.

[9] R. K. Gautam, S. Ray, S. C. Sharma, S. C. Jain, and R. Tyagi, "Dry sliding wear behavior of hot forged and annealed Cu-Cr-graphite in-situ composites," *Wear*, vol. 271, no. 5-6, pp. 658–664, 2011.

[10] J. Sankar, S. S. Kumar, P. Balamurugan, S. Kumar, S. A. Saleem, and S. V. Krishna, "Fabrication and corrosion studies of bronze based composite prepared through powder metallurgy route," *Material Today Proceeding*, vol. 50, no. 5, pp. 1067–1070, 2022.

[11] R. Venkatesh, C. R. Kannan, S. Manivannan et al., "Synthesis and experimental investigations of tribological and corrosion performance of AZ61 magnesium alloy hybrid composites," *Journal of Nanomaterials*, vol. 2022, Article ID 6012518, 12 pages, 2022.

[12] S. Priya Karjala, V. K. K. Rajammal, S. Gopi, R. Ravi, D. Chockalingam, and M. C. Muthukaruppan, "Influence of IPNS (vinylester/epoxy/polyurethane) on the mechanical properties of glass/carbon fiber reinforced hybrid composites," *IIUM Engineering Journal*, vol. 23, no. 1, pp. 339–348, 2022.

[13] R. Venkatesh, N. Karthi, N. Kawin et al., "Synthesis and adsorbent performance of modified biochar with ag/MgO nanocomposites for heat storage application," *Adsorption Science & Technology*, vol. 2022, article 7423102, pp. 1–14, 2022.

[14] K. Karthikeyan, V. Mariappan, P. Kalidoss et al., "Preparation and thermal characterization of capric-myristic acid binary eutectic mixture with silver-antimony tin oxide and silver-graphane nanoplatelets hybrid-nanoparticles as phase change material for building applications," *Materials Letter*, vol. 328, article 133086, 2022.

[15] A. M. Kovalchenko, O. I. Fushchich, and S. Danyluk, "The tribological properties and mechanism of wear of Cu-based sintered powder materials containing molybdenum disulfide and molybdenum diselenite under unlubricated sliding against copper," *Wear*, vol. 290-291, pp. 106–123, 2012.

[16] M. Vamsi Krishna and M. Xavior Anthony, "An investigation on the mechanical properties of hybrid metal matrix composites," *Procedia Engineering*, vol. 97, pp. 918–924, 2014.

[17] P. S. Reddy, R. Kesavan, and B. Vijaya Ramnath, "Investigation of mechanical properties of aluminium 6061-silicon carbide, boron carbide metal matrix composite," *Silicon*, vol. 10, no. 2, pp. 495–502, 2018.

[18] C. Ramesh Kannan, R. Venkatesh, M. Vivekanandan et al., "Synthesis and characterization of mechanical properties of AA8014 + $Si_3N_4$/ $ZrO_2$ hybrid composites by stir casting process," *Advances in Materials Science and Engineering*, vol. 2022, Article ID 9150442, 11 pages, 2022.

[19] A. Mohan and S. Poobal, "Crack detection using image processing: a critical review and analysis," *Alexandria Engineering Journal*, vol. 57, no. 2, pp. 787–798, 2018.

[20] M. Uthayakumar, V. Manikandan, N. Rajini, and P. Jeyaraj, "Influence of redmud on the mechanical, damping and chemical resistance properties of banana/polyester hybrid composites," *Material Design*, vol. 64, pp. 270–279, 2014.

[21] C. S. Ramesh, R. Noor Ahmed, M. A. Mujeebu, and M. Z. Abdullah, "Development and performance analysis of novel cast copper-SiC-Gr hybrid composites," *Material Design*, vol. 30, no. 6, pp. 1957–1965, 2009.

[22] A. K. Kanayo and O. B. Ufuoma, "Mechanical properties, wear and corrosion behavior of copper matrix composites reinforced with steel machining chips," *International Journal of Engineering Science and Technology*, vol. 19, no. 3, pp. 1593–1599, 2016.

[23] K. Chu, C. C. Jia, L. K. Jiang, and W. S. Li, "Improvement of interface and mechanical properties in carbon nanotube reinforced Cu-Cr matrix composites," *Material Design*, vol. 45, pp. 407–411, 2013.

[24] T. Rajmohan and K. Palanikumar, "Application of the central composite design in optimization of machining parameters in drilling hybrid metal matrix composites," *Measurement*, vol. 46, no. 4, pp. 1470–1481, 2013.

[25] R. Chandramouli, T. K. Kandavel, D. Shanmugasundaram, and T. Ashok Kumar, "Deformation, densification, and corrosion studies of sintered powder metallurgy plain carbon steel preforms," *Material Design*, vol. 28, no. 7, pp. 2260–2264, 2007.

[26] R. Venkatesh, P. R. Sekaran, K. Udayakumar, D. Jagadeesh, K. Raju, and M. B. Bayu, "Adsorption and photocatalytic degradation properties of bimetallic Ag/MgO/biochar nanocomposites," *Adsorption Science & Technology*, vol. 2022, article 3631584, pp. 1–14, 2022.

[27] R. Orozco-Cruz, "In situ corrosion study of copper and copper-alloys exposed to natural seawater of the Veracruz port (Gulf of Mexico)," *International Journal of Electrochemical Science*, vol. 12, pp. 3133–3152, 2017.

[28] D. Saber, R. Abdel-Karim, A. A. Kandel, and K. A. el-Aziz, "Corrosive wear of alumina particles reinforced Al–Si alloy composites," *Physics of Metals and Metallography*, vol. 121, no. 2, pp. 188–194, 2020.

[29] C. Suryanarayana and A. A. Nasser, "Mechanically alloyed composites," *Progress in Material Science*, vol. 58, pp. 383–502, 2013.

[30] A. Mohana Krishnan, P. Laxmanan, and R. Venkatesh, "Salt spray corrosion study on aluminium metal matrix composites (AMMCs) prepared by powder metallurgy route," *Materials Today Proceedings*, vol. 62, no. 2022, pp. 1954–1957, 2022.

[31] J. I. Iribarren, F. Liesa, C. Alemán, and E. Armelin, "Corrosion rate evaluation by gravimetric and electrochemical techniques applied to the metallic reinforcing structures of a historic building," *Journal of Cultural Heritage*, vol. 27, pp. 153–163, 2017.

[32] A. Sobhanadri, G. Senthilkumar, M. Vivekanandan, and R. Venkatesh, "A CFD investigation and heat transfer augmentation of double pipe heat exchanger by employing helical baffles on shell and tube side," *Thermal Science*, vol. 26, no. 2A, pp. 991–998, 2022.

[33] A. Fathy, F. Shehata, M. Abdelhameed, and M. Elmahdy, "Compressive and wear resistance of nanometric alumina reinforced copper matrix composites," *Material Design*, vol. 36, pp. 100–107, 2012.

[34] A. W. Coats and J. P. Redfern, "Thermogravimetric analysis: a review," *Analyst (Cambridge, UK)*, vol. 88, no. 1053, pp. 906–924, 1963.

[35] A. Mohana Krishnan, M. Dineshkumar, and R. Venkatesh, "Evaluation of mechanical strength of the stir casted aluminium metal matrix composites (AMMCs) using Taguchi method," *Materials Today Proceedings*, vol. 62, no. 2022, pp. 1943–1946, 2022.